

Implantation depth of size-selected silver clusters into graphite

This article has been downloaded from IOPscience. Please scroll down to see the full text article.

2002 J. Phys.: Condens. Matter 14 L185

(<http://iopscience.iop.org/0953-8984/14/8/102>)

View [the table of contents for this issue](#), or go to the [journal homepage](#) for more

Download details:

IP Address: 171.66.16.27

The article was downloaded on 17/05/2010 at 06:11

Please note that [terms and conditions apply](#).

LETTER TO THE EDITOR

Implantation depth of size-selected silver clusters into graphite

D J Kenny^{1,3}, R E Palmer¹, C F Sanz-Navarro² and R Smith²

¹ Nanoscale Physics Research Laboratory, School of Physics and Astronomy, The University of Birmingham, Birmingham, B15 2TT, UK

² School of Mathematics and Physics, Loughborough University, Loughborough, Leicestershire, LE11 3TU, UK

E-mail: R.E.Palmer@bham.ac.uk

Received 14 November 2001

Published 15 February 2002

Online at stacks.iop.org/JPhysCM/14/L185

Abstract

We have investigated the implantation of size-selected Ag_7^- clusters into the graphite surface as a function of kinetic energy (E) from 1.0 to 5.5 keV, via scanning tunnelling microscopy together with molecular dynamics simulations. By utilizing thermal oxidation of the graphite surface to expand laterally the defects created via implantation, we find that the cluster implantation depth is proportional to \sqrt{E} and hence the velocity of the bombarding cluster. By careful control of the oxidation temperature, we also demonstrate that even moderate temperatures (923–1123 K), considerably lower than the melting point of graphite (4450 K), lead to significant annealing of the defects formed through cluster impact, accounting for the shape of the experimental depth distributions observed.

There is considerable interest in the interaction of small metal clusters with surfaces, primarily due to their size-dependent properties. For example, arrays of size-selected clusters have been shown to display size-specific catalytic activity [1, 2]. However, after low-energy deposition upon a surface, clusters can often diffuse and aggregate to form larger clusters or islands, thus destroying the initial cluster size distribution [3, 4]. Low temperatures are one route for reducing cluster diffusion, but this restricts further experimental studies, e.g. of chemical reactivity and catalysis. To create a monodispersed array of size-selected clusters, which is stable at room temperature, may thus require that the clusters are pinned to [5], or implanted within [6], the surface, to prevent diffusion and aggregation. This goal demonstrates the need to understand energetic cluster–surface interactions.

Recent scanning tunnelling microscopy (STM) studies by Hall *et al* [6] have investigated the impact event, and resultant defect formation, when small Ag_n^- clusters ($n = 1-7$) are

³ Present address: Micromass UK Limited, Floats Road, Wythenshawe, Manchester M23 9LZ, UK.

deposited onto the (model) graphite surface. XPS measurements of the same system by Yamaguchi *et al* [7] have revealed three distinct energy regions: soft landing, rebounding and implantation. This work also showed that the cluster–surface interaction was dependent upon the cross-sectional area of the cluster, consistent with previous molecular dynamics (MD) simulations of larger Ag_n clusters ($n = 20\text{--}200$) by Carroll *et al* [8], which examined implantation depths over a wide range of energies (E), 0.75–6 keV. The theoretical study revealed that large clusters, implanted into the graphite surface, remained more or less intact, although amorphous, and came to rest at the bottom of an open tunnel or ‘well’, while the cluster implantation depth (D) scaled as $D \propto E/N^{2/3}$, where N is the number of atoms in the cluster. Note also that this kind of structure offers a possible future direction for forming catalytical materials with enhanced thermal stability.

Direct STM measurement of the depth of such well structures presents a significant challenge, because of the large STM tip diameter in comparison with that of the well. However, several groups have now successfully measured the implantation depths of Ag_7^- [9], $\text{Ta}_{1,2,4,9}^+$ [10] and C_{60}^+ [11] clusters in graphite by exploiting the anisotropic chemical reactivity of the graphite surface through an oxidative etching step, which ‘expands’ the wells laterally to form shallow pits. Similar etch pits created from natural surface defects, and of a single monolayer depth, have also been exploited as ‘molecular corrals’ to control the growth of organic molecular films [12, 13] and clusters [14].

In this letter we present experimental results and MD simulations which systematically investigate the scaling of the implantation depth as a function of the kinetic energy of the cluster. In the case of small (Ag_7^-) clusters, the implantation depth is found to be linearly dependent upon the *velocity* (i.e. $D \propto v$) of the cluster, rather than its kinetic energy (i.e. $D \propto v^2$) as has been found in MD simulations for larger Ag_n ($n = 20\text{--}200$) clusters. We also demonstrate that the moderate temperature (650 °C) associated with the oxidative etching process can partially heal the defects formed through cluster impact, leading to shallower than expected etch pits.

Ag_7^- clusters were created using a Cs^+ ion sputter source [15] and deposited in high vacuum (1×10^{-7} mbar) onto graphite samples that were cleaved immediately prior to insertion into vacuum, but which had not been subjected to any further cleaning procedures. After cluster deposition, the samples were removed from the vacuum chamber and oxidized in a tube furnace at 650 °C for periods of 3–5 min under ambient atmospheric conditions. After allowing the samples to cool, a benchtop STM (DME Rasterscope 4000) was used to investigate the depth of the resultant etch pits. Typical operating conditions for the STM were a sample bias of +0.4 V and a tunnelling current of 0.4 nA, using mechanically cut Pt/Ir tips.

The experimental results were compared with MD simulations [16], in which the area of the graphite substrate was $50 \text{ \AA} \times 50 \text{ \AA}$, and a total of 16 graphite layers were included. All simulations were run for 2.5 ps, with a time step of 0.75 fs. The short impact time of 2.5 ps was chosen because it allows us to run a number of different trajectories to get better statistics; furthermore, due to the layered structure of graphite, the cluster vibrates for a very long period trapped between the graphite layers and it was noted that the midpoint of the first oscillation is very close to the mean position during much longer simulations [17]. The initial configuration of the (neutral) Ag_7 cluster in the simulations was found by applying a genetic algorithm [18] to seven Ag atoms interacting with each other through a many-body potential function parametrized by Ackland *et al* [19]. This same potential was also used to model the Ag–Ag interaction during the impact simulation. The covalent C–C interaction was modelled by a many-body Brenner potential [20], but an additional Lennard-Jones potential [16] was used between atoms that were not linked by covalent bonds to simulate the Van der Waals interaction between graphite layers. The Ag–C interaction was modelled by a Morse potential [21].

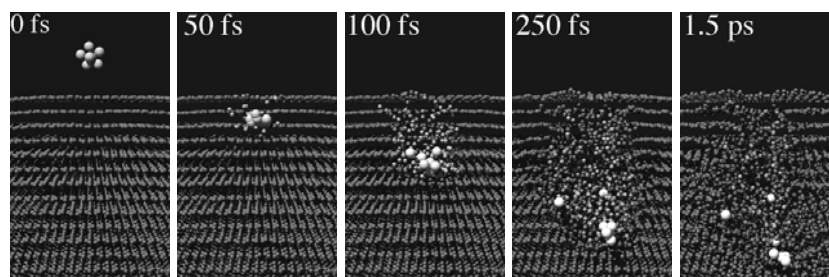


Figure 1. MD simulation snapshots, shown in cross section, following the progress of an Ag_7 (neutral) cluster implanting into the graphite surface at 4 keV.

Additionally, the Ag–C potential was splined to the two-body ZBL screened Coulomb potential for high interaction energies [22]. The temperature of the system was initially equilibrated to 300 K before the start of the simulation by employing a thermostat [23], but this was switched off during the impact. In total, seven different impact energies were modelled within the range 0.5–5.0 keV; each energy was repeated 12 times (a combination of three different cluster orientations and four different impact sites).

Figure 1 displays five snapshots from an MD simulation of the deposition of a (neutral) Ag_7 cluster onto the graphite surface at an energy of 4 keV (equivalent to a velocity of 32 km s^{-1} , 72 000 mph). After 50 fs the cluster has already broken through the first two graphite layers, pushing several interstitial atoms between the layers, and has begun to damage the third layer. At this point, whilst no longer retaining its original pentagonal bi-pyramid form, the cluster is still relatively intact. After 100 fs, the cluster has penetrated further into the bulk and has passed through a total of five graphite layers. It is also evident that the cluster has started to fragment and that the passage of the cluster has resulted in the formation of an amorphous carbon channel in the substrate. At 250 fs the cluster has almost come to rest, after penetrating ten layers. A five-atom ‘core’ derived from the original cluster still remains, but two atoms have been stripped away by the impact process. Finally, the cluster is trapped between the tenth and 11th layers and starts to vibrate around an equilibrium position.

Figure 2 is an STM image of a graphite surface after implantation of Ag_7^- clusters at 4 keV and subsequent oxidative etching. The resultant etch pits are typically polygonal in shape, reflecting the (hexagonal) atomic structure of the surface, and show a characteristic range of depths. Also visible are several shallow (one monolayer (ML)) pits, generated from naturally occurring surface defects. By measuring the depth of each etch pit using the STM (see line profile in figure 2), it is possible to produce a plot of the frequency of occurrence of each depth for a particular implantation energy.

Figures 3(a)–(c) show representative experimental and MD simulation data for implantation energies of (a) 1 keV, (b) 3 keV and (c) 5 keV. The experimental results are plotted as \circ ; the solid curves represent a Gaussian fit to the data in each case. The MD results are shown as shaded bars. In total, 11 energies between 1.0 and 5.5 keV have been investigated experimentally. By imaging regions of each sample that were not exposed to the cluster beam, it was possible to find the ‘background count’ of pits arising from natural defects and subtract them from the raw data, as has been described previously [9]. Examining figures 3(a)–(c) in turn, there is a clear upward shift in the experimental etch pit depths with increasing energy. Additionally, the experimental data show a broad distribution of depths, corresponding to an approximately Gaussian distribution (although in figure 3(a), at 1 keV, the Gaussian form is effectively truncated below 1 ML). In contrast, the MD simulation results

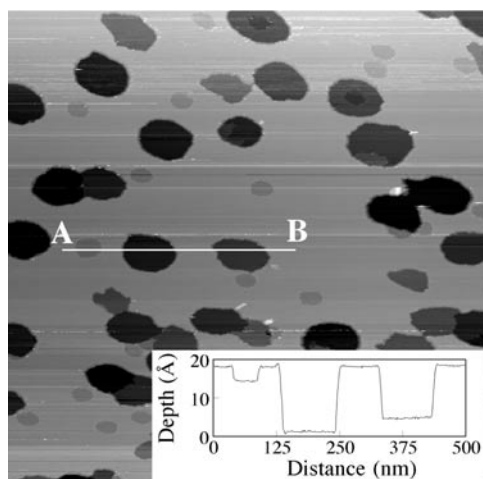


Figure 2. STM image of a graphite surface ($1\ \mu\text{m} \times 1\ \mu\text{m}$) after Ag_7^- implantation at 4 keV and oxidative etching at 650°C for 3 min. Etch pits of various depths can be seen; deeper pits are a result of cluster impact, shallow (1 ML deep) pits are due to natural defects. The inset shows a height profile along the line indicated (A–B). The tunnelling parameters used were +0.4 V and 0.4 nA.

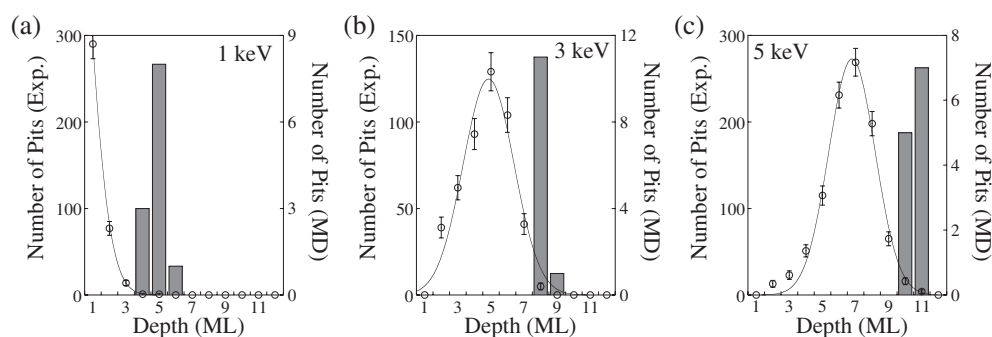


Figure 3. Histograms displaying experimental (\circ) and MD simulation (bars) distributions of implantation depths for cluster impact energies of (a) 1 keV, (b) 3 keV and (c) 5 keV. The experimental distributions are approximately Gaussian in nature, although the distribution is effectively truncated in (a).

show a much narrower distribution of depths, which coincides in each case with the upper wing of the experimental distribution.

Previous MD simulations have also indicated that the implantation depths of Ta_{1-9} [10,24] and C_{60} [25] clusters in graphite are larger than the peak depths derived experimentally from the oxidative etching technique. It was suggested that the high temperature utilized in the etching process partly anneals the defects created by the implanting cluster, i.e. that the defects are partially healed before oxidation takes hold. Such a process could reduce the depth of many etch pits and give rise to the observed broad depth distribution, although until now there have been no specific experiments which have directly explored the proposed nanoscale annealing of the graphite defects.

Figure 4 shows three histograms of etch pit depths obtained from graphite samples bombarded with Ag_7^- clusters at 5 keV prior to etching. The white bars relate to samples

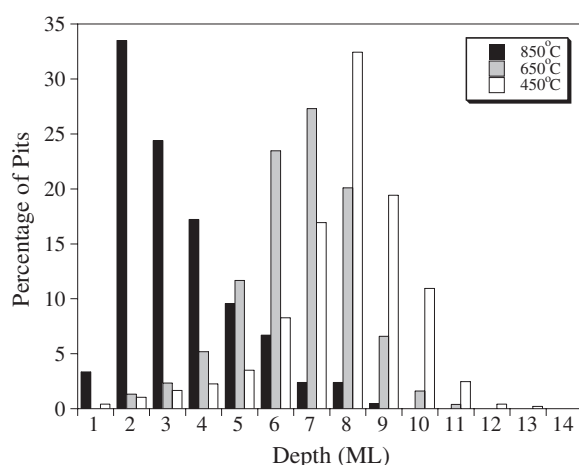


Figure 4. Histograms of experimental etch pit depths after Ag_7^- bombardment at 5 keV followed by oxidative etching at 450 °C for 1.5 h (white bars), oxidative etching at 650 °C for 3 min (grey bars) and annealing in UHV at 850 °C for 3 min followed by oxidative etching at the normal temperature of 650 °C (black bars).

which were oxidatively etched at the lower than normal temperature of 450 °C for a period of 1.5 h, whereas the black bars correspond to samples annealed in UHV at 850 °C for 3 min prior to etching at the normal temperature of 650 °C. The grey bars relate to samples etched at 650 °C in the usual manner. It is immediately apparent that the three histograms display quite different distributions of etch pit depths. Etching at 450 °C, compared with 650 °C, has resulted in an overall increase of ≈ 1 ML in the depth distribution, whereas pre-annealing at 850 °C leads to a major decrease in depth of 5–6 ML. These results clearly indicate that even the moderate temperatures used during oxidation are sufficient to significantly heal the damage formed by the implanted clusters, giving rise to the shallower implantation depths recorded experimentally in comparison with the MD simulations.

The correspondence between the upper end of the experimental distributions, figure 3, and the corresponding MD implantation depths in figure 3 leads us to propose that the upper region corresponds to defects which are largely unaffected by the annealing process, and hence represent the ‘true’ implantation depths. To obtain quantitative values for this true implantation depth, we have therefore taken an average value from those pits that lie beyond two standard deviations from the peak of each distribution. Figure 5 compares the experimental results so obtained with the corresponding values from the MD depth distributions.

Plotting both sets of data as a function of cluster kinetic energy, E , revealed that the implantation depth varies as \sqrt{E} . By plotting the implantation depth in figure 5 as a function of the cluster velocity, v , we therefore obtain good linear fits. The experimental data are represented in the figure by \circ and a full line, while the MD results are plotted using \square and a dashed line. The experimental and theoretical sets of data agree well within their representative error limits, although we note a slight divergence at lower velocities. The resulting linear fits therefore have slightly different gradients and y -intercepts. The negative (depth) y -intercepts of (-7.0 ± 2.1) and (-3.66 ± 0.54) Å, respectively, for the experimental and MD data correspond to soft landing of the cluster, so that it sits upon the surface; the depth is measured with respect to the outermost layer of carbon atoms. The dependence of the implantation depth on the cluster velocity, found in both the experimental and simulated

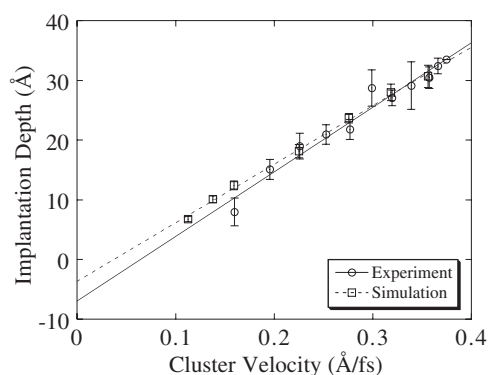


Figure 5. Plot showing implantation depths, as a function of cluster impact velocity, for Ag_7^- found experimentally (\circ) and from MD simulation (\square). Linear fits to the data are displayed for both the experimental (—) and simulated (---) data.

distributions, is a rather unexpected result, since earlier MD studies of larger silver clusters determined that the implantation depth varies linearly with the cluster kinetic energy, E , [8]. The scaling with velocity does, however, agree with previous investigations of the implantation of C_{60}^+ ions into the graphite surface. The crossover from velocity scaling to kinetic energy scaling as the cluster size increases is intriguing and remains to be understood.

We have systematically explored the implantation of size-selected, Ag_7^- , clusters into the graphite surface, leading to the formation of well defined etch pits after subsequent annealing in oxygen. Two principal results have been obtained. (i) We have established that even the moderate temperatures (650°C) associated with the oxidative etching of graphite also tend to anneal the defects arising from cluster impact, resulting in shallower and wider depth distributions than predicted by MD simulations. (ii) Further, by considering only the deepest pits, we have been able to compare directly experimental and MD simulation values for the implantation depth and hence determine that the implantation depth of Ag_7^- varies as a function of the velocity of the cluster rather than its energy.

We would like to thank the Engineering and Physical Sciences Research Council (EPSRC) for financial support of this work and the award of a studentship to DJK. We are also very grateful to S C Weller and M Couillard for their assistance in producing the cluster-implanted samples.

References

- [1] Sanchez A, Abbet S, Heiz U, Schneider W D, Hakkinen H, Barnett R N and Landman U 1999 *J. Phys. Chem. A* **103** 9573
- [2] Valden M, Lai X and Goodman D W 1998 *Science* **281** 1647
- [3] Goldby I M, Kuipers L, von Issendorff B and Palmer R E 1996 *Appl. Phys. Lett.* **69** 2819
- [4] Carroll S J, Seeger K and Palmer R E 1998 *Appl. Phys. Lett.* **72** 305
- [5] Carroll S J, Pratontep S, Streun M, Palmer R E, Hobday S and Smith R 2000 *J. Chem. Phys.* **113** 7723
- [6] Hall S G, Nielsen M B and Palmer R E 1998 *J. Appl. Phys.* **83** 733
- [7] Yamaguchi W, Yoshimura K, Tai Y, Maruyama Y, Iarashi K, Tanamura S and Murakami J 2000 *J. Chem. Phys.* **112** 9961
- [8] Carroll S J, Nellist P D, Palmer R E, Hobday S and Smith R 2000 *Phys. Rev. Lett.* **84** 2654
- [9] Kenny D J, Weller S, Couillard M, Palmer R E, Sanz-Navarro C F and Smith R 2001 *Eur. Phys. J. D* **16** 115
- [10] Reimann C T, Andersson S, Brühwiler P A, Mårtensson N, Olsson L, Erlandsson R, Henkel M and Urbassek H M 1998 *Nucl. Instrum. Methods B* **140** 159

- [11] Bräuchle G, Richard-Schneider S, Illig D, Rockenberger J, Beck R D and Kappes M M 1995 *Appl. Phys. Lett.* **67** 52
- [12] Patrick D L, Cee V J and Beebe T P 1994 *Science* **265** 231
- [13] Stevens F, Buehner D and Beebe T P 1997 *J. Phys. Chem. B* **101** 6491
- [14] Hövel H, Becker Th, Betta A, Reihl B, Tschudy M and Williams E J 1997 *J. Appl. Phys.* **81** 154
- [15] Hall S G, Nielsen M B, Robinson A W and Palmer R E 1997 *Rev. Sci. Instrum.* **68** 3335
- [16] Smith R and Beardmore K M 1996 *Thin Solid Films* **272** 255
- [17] Sanz-Navarro C F, Smith R, Kenny D J, Pratontep S and Palmer R E 2001 *Phys. Rev. B* at press
- [18] Hobday S and Smith R 1997 *J. Chem. Soc. Faraday Trans.* **93** 3919
- [19] Ackland G J, Tichy G, Vitek V and Finnis M W 1987 *Phil. Mag. A* **56** 736
- [20] Brenner D W 1990 *Phys. Rev. B* **42** 9458
- [21] Rafii-Tabar H, Kamiyama H and Cross M 1997 *Surf. Sci.* **385** 187
- [22] Ziegler J F, Biersack J P and Littmark U (ed) 1985 *The Stopping and Ranges of Ions in Solids* (New York: Pergamon)
- [23] Berendsen H J C, Postma J P M, van Gunsteren W F, DiNola A and Haak J R 1984 *J. Chem. Phys.* **81** 3684
- [24] Henkel M and Urbassek H M 1998 *Nucl. Instrum. Methods B* **145** 503
- [25] Webb R P, Kerford M, Kappes M and Bräuchle G 1997 *Nucl. Instrum. Methods B* **122** 318